

# **1.**

## **Damage Scenarios Simulation for Seismic Risk Assessment in Urban Zones**

Alex H. Barbat, M.EERI, Fabricio Yépez Moya, and José A. Canas

A methodology for simulating seismic damage of unreinforced masonry buildings for seismic risk assessment of urban areas is presented in this paper. The methodology is based on the Italian vulnerability index and on the results of a post-earthquake damage survey study whose main result was an observed vulnerability function. The Monte Carlo method was then used to simulate damage probability matrices, fragility curves and vulnerability functions, all of which are the basis of a seismic risk study. The simulation process required the generation of thousands of hypothetical buildings, the analysis of their seismic behaviour and probabilistic studies of the computed results. As an example, probable damage scenarios were developed for an urban zone of Barcelona.

### **INTRODUCTION**

The damage produced by earthquakes in structures and the economic and social consequences, have stimulated studies on seismic risk of structures and in particular the risk of old buildings for which a high degree of damage could be expected. In this paper, the *seismic risk* is defined as the convolution of the following factors (Sandi 1986, Yépez *et al.* 1995):

- (a) The *seismic hazard* of the site, defined as the probability of occurrence of an earthquake of a given intensity within a given period of time.
- (b) The *seismic vulnerability*, defined by the degree of damage observed in structures as a result of the occurrence of an earthquake of a given intensity.
- (c) The *cost* of the structures.

A suitable mechanism for seismic risk mitigation is vulnerability reduction and, therefore, its evaluation is very important. The expected result of a seismic vulnerability study is the degree of damage that a structure with a specified typology would suffer,

---

(AHB, FYM, JAC) ETSECCPB, Technical University of Catalonia, c/Gran Capitán s/n, 08034 Barcelona, Spain

when subjected to a seismic action with specified characteristics. It can be defined by means of: 1) *damage probability matrices*, which express in a discrete form the conditional probability  $P[D = j|i]$  to obtain a damage level  $j$ , due to an earthquake of  $i$  size; and 2) *vulnerability functions*, which are relations expressing the vulnerability in a continuous form, as a function of certain parameters that describe the size of the earthquake (Yépez, Barbat and Canas 1994). Damage probability matrices and vulnerability functions can be obtained by means of statistical studies of damage observed after earthquakes—observed vulnerability—, or by simulation of the results using mechanical and mathematical models of structures—calculated vulnerability—. However, it has to be pointed out that there is a lack of vulnerability studies in many countries with significant seismicity.

Depending on the way vulnerability is expressed, the *specific risk*  $S$  can be evaluated in the following two manners (Yépez, Barbat and Canas 1994):

- *Using damage probability matrices*

$$S = \sum_j \sum_i P[D = j|i] P[i] \quad (1)$$

where  $P[D = j|i]$  is the conditional probability of occurrence of a damage level  $j$ , due to an earthquake of intensity  $i$  and  $P[i]$  is the probability of occurrence of that earthquake for a specific return period. Thus, the specific risk  $S$  can be associated, for example, with the same return period as the seismic hazard.

- *Using vulnerability functions*

$$F(\bar{d}) = \int_0^{\bar{d}} \int_0^{I_{\max}} f(d|I) f(I) dI dd \quad (2)$$

$$S = F(d_{\max}) \quad (3)$$

where  $F(\bar{d})$  is the cumulative distribution function for a damage level  $d = \bar{d}$ , whenever all the involved variables can be considered as random, independent and continuous in their definition range.  $f(d|I)$  is the conditional density function of damage over the intensity  $I$  and  $f(I)$  is the density function of annual intensity. Hence, the specific seismic risk  $S$  is expressed by Equation (3) as the cumulative distribution function for the maximum damage  $d_{\max}$ .

The aim of this study is to perform a seismic damage simulation for unreinforced masonry buildings, to propose a calibration procedure of the simulated vulnerability functions using a post-earthquake damage survey and, by means of a probabilistic analysis, to deduce damage probability matrices and fragility curves applicable to Spain. The methodology is then applied to an urban area of Barcelona, the “Eixample”, to obtain probable damage scenarios.

## THE VULNERABILITY INDEX METHOD

For the evaluation of the seismic vulnerability of buildings in an urban zone, the *vulnerability index method* (GNDT 1986) has been chosen. This method was developed and extensively applied to several seismic zones in Italy and was based on a great amount of damage survey data. The method identifies the most important parameters controlling the damage in buildings caused by seismic loads. Thus, the study of the plant and elevation configuration, the type of foundation, structural and nonstructural elements, the state of preservation and the type and quality of materials are qualified individually on a numerical scale, affected by weights  $W_i$  which try to emphasize the relative importance of the different parameters involved. From the obtained values, the method makes an overall qualification of the buildings by means of a *vulnerability index*  $I_v$  on a scale ranging from 0 to 382.5 (Benedetti and Petrini 1984). Table 1 shows a list of the eleven parameters considered in the qualification of the structures, the values of the corresponding possible qualification coefficients  $K_i$  in accordance with quality conditions (from A —optimal— to D —unfavourable—) and the weighting factors  $W_i$  assigned to each parameter by Benedetti and Petrini (1984). The global vulnerability index of each building is evaluated using the formula

$$I_v = \sum_{i=1}^{11} K_i W_i \quad (4)$$

TABLE 1

Numerical scale of vulnerability index  $I_v$  (Benedetti and Petrini 1984).

$i$	<i>Parameter</i>	$K_iA$	$K_iB$	$K_iC$	$K_iD$	$W_i$
1	Resistance system organization	0	5	20	45	1.0
2	Resistance system quality	0	5	25	45	0.25
3	Conventional resistance	0	5	25	45	1.5
4	Retaining walls and foundation	0	5	25	45	0.75
5	Floor system	0	5	15	45	1.0
6	Plant configuration	0	5	25	45	0.5
7	Elevation configuration	0	5	25	45	1.0
8	Maximum distance between walls	0	5	25	45	0.25
9	Roof type	0	15	25	45	1.0
10	Nonstructural elements	0	0	25	45	0.25
11	Preservation state	0	5	25	45	1.0

The vulnerability index can be taken as a parameter that helps to assess the lack of building safety under seismic loads. However, it does also permit the definition of *vulnerability functions* by relating the vulnerability index  $I_v$  to a global damage index  $D$  of buildings having the same typology, for the same macroseismic intensity  $I$ . The

damage observed in buildings after an earthquake, or the computer simulation of the structural damage using mechanical and mathematical models, permits the deduction, by means of probabilistic methods, of these specific functions. A global damage index  $D$ , characterizing the structural state of a complete building after an earthquake, can be defined as the weighted combination of values describing the post-earthquake state of the different structural components such as the vertical and horizontal elements, inner walls and nonstructural components. The final result is a damage index with values ranging between 0% and 100%. Nevertheless, several seismic vulnerability studies based on different methods conclude that the vulnerability functions obtained in different countries are not completely reliable (Yépez, Barbat and Canas 1994). Therefore, specific vulnerability functions must be obtained to consider, for example, different construction techniques and different types of manpower. This is only possible using and processing the information obtained from post-earthquake studies carried out in each analyzed region.

In order to obtain observed functions for Spain, which relate vulnerability to the global damage indices of buildings (observed vulnerability functions), a post-earthquake study has been performed on two crustal earthquakes occurred in southern Spain on December 23, 1993 and on January 4, 1994. The epicenters were located in the Almería region: the first near the towns of San Roque and Berja and the second about 20 km off the coast from Almería and Baños. Their focal depth was 10-15 km. The maximum evaluated intensity in the critical sites was VII on the Medvedev-Sponheuer-Karnik (MSK) scale used in Spain and in other European countries (*European Seismological Commission*, 1993).

The study began by surveying the damage to several masonry and concrete structures (Goula *et al.* 1994). The type and extent of the damage were analyzed and classified for each structural and nonstructural part of damaged building and correlated with the damage index defined by the Italian methodology. At the same time, their vulnerability was evaluated according to the same methodology. Once the vulnerability and the damage indices for each studied building had been determined, a statistical analysis was performed, yielding the vulnerability function corresponding to the level of intensity assigned to that region (VII MSK). The function fitted to the data was

$$D = 2.76 \times 10^{-6} I_v^3 - 5.0335 \times 10^{-4} I_v^2 + 0.02959505 I_v - 0.08823776 = 0 \quad (5)$$

Figure 1 shows the survey data, the polynomial regression function and, as a comparison, the functions proposed by Angeletti *et al.* (1988) for the VI, VII and VIII intensities on the Mercalli-Cancani-Sieberg (MCS) scale used in Italy. The comparison is possible due to the similarity between the intensity degrees defined by the MCS and MSK scales. This was the first observed vulnerability function obtained from a post-earthquake study in Spain and, possibly, the first ever obtained outside Italy using the vulnerability index method (Yépez, Barbat and Canas 1994).

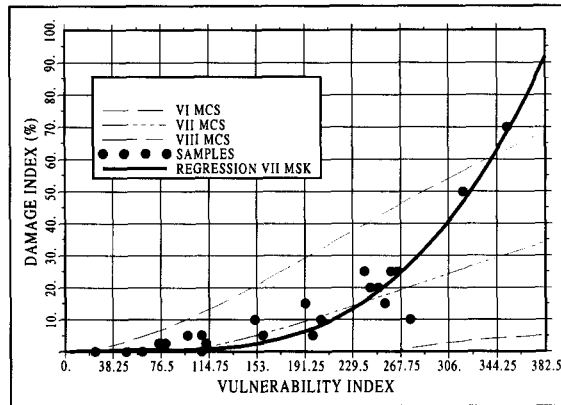


Figure 1 Vulnerability function observed in Spain for VII MSK intensity level (Yépez, Barbat and Canas 1994). The functions proposed by Angeletti *et al.* (1988) are represented by discontinuous lines.

### SIMULATION AND CALIBRATION OF THE VULNERABILITY FUNCTIONS

The survey of structures damaged in the Almería region provided only one vulnerability function, corresponding to the intensity VII MSK assigned to the earthquake in that region. With the aim of obtaining vulnerability functions for other intensity levels, a computer simulation process was necessary. The first step of this process was the simulation of the vulnerability function for intensity VII MSK and its calibration with the observed vulnerability function of Figure 1. Studies on calculated vulnerability have been performed previously by using structural models based on experimental tests, for example, those of Manfredi, Mazzolani and Masi (1992) or Abrams (1992), even without the necessity of possessing survey data from post-earthquake studies. In this section, the simulation and calibration of the vulnerability functions is performed by using the Abrams (1992) model.

Masonry is a non-homogeneous and non-isotropic material. This aspect, together with the variety of masonry types and constructive typologies in use, makes structural modelling a difficult problem. The anisotropy of the material, whenever the shape of the members is sufficiently regular, does not seriously affect the modelling process. Conversely, if the structural members are irregular, the most frequent situation, especially for old buildings, the models are very complex. By taking into account all these factors, it is possible to describe the behaviour of a masonry wall by using models with different difficulty levels. The selected model depends on certain knowledge about the characteristics of the applied loads, the experimental parameters required by the model and, of course, depends on the required aim of the study (Manfredi, Mazzolani and Masi 1992).

Methods based on the calculated vulnerability use structural models able to reproduce the inelastic cyclic strains experienced by the elements during the application of seismic loads. These methods use damage indices to relate the computed structural response to the damage that has occurred in the structural elements or in the entire structure. These are able to evaluate only the capacity of the degraded structure to resist seismic loads and, therefore, it is difficult to relate them to the actual damage observed in buildings during an earthquake. Obviously, an index based on the actual damage is not only more reliable, but also a better measure of the total economic losses. On the other hand, the use of calculated vulnerability methods to simulate the behaviour of a complete urban zone is a practically impossible task and, for this reason, its application is restricted to individual structures (Yépez, Barbat and Canas 1994). Thus, due to the nature and the objectives of this study, it was not possible to apply sophisticated models since, as it is shown further on, it was necessary to simulate thousands of buildings with random characteristics. Therefore, it was necessary to use a more simple model which was able to describe properly the inelastic behaviour observed in experimental studies.

From the few existing methods for evaluating the behaviour of masonry elements, the model developed by Abrams (1992) has been chosen. It was applied to the structure modelled as a shear building—in the case of stiff floors—or to the overall structure modelled as a shear wall—in the case of more flexible floors—. The Abrams model for unreinforced masonry walls takes into account the increment of the lateral structural strength after the initial cracking, a fact that allows higher strength levels than required by most seismic building codes to be reached. The model analyses the types of failure controlling the wall behaviour caused by the simultaneous action of flexural-compressional and shear stresses. Finally, it evaluates the maximum resistance to seismic loads of the walls on each floor. This makes it possible to calculate damage indices of the structure using relations between the actual shear stress state produced by the seismic action in the structure and the shear stress state corresponding to the collapse.

The application of the Abrams method only takes into account the capacity/demand relationship of the masonry panel strength. This aspect requires certain assumptions to be made on the structural behaviour. Moreover, some special effects such as weak floor-to-wall connections, irregularity of masonry units and badly aligned panels are omitted in the analysis. To take into account all structural details, it is necessary to perform more refined analyses, using, for example, finite element models. Obviously, the application of a more complex model requires very extensive computer calculations, impossible to perform if thousands of buildings are to be analyzed. Nevertheless, it has to be pointed out that the information that can be obtained by using the chosen model is sufficient for the main objective of the present study, which was the seismic risk assessment for a complete urban area. Then, for a specific and vulnerable structure, it is possible to apply, if required, a more sophisticated analysis. Additionally, because of the lack of resolution, a characteristic of most seismic hazard studies, and due to the input data required by the Abrams model, the seismic action was defined using the response spectra of the Spanish Seismic Code.

The relation proposed by Chung and Shinozuka (1988) has been used to determine the global damage index of the structure, which is defined as a weighted sum of the damage indices of each individual floor, where the weights are higher if the floor is lower. The proposed equation is

$$D = \sum_{i=1}^n \left( \frac{n+1-i}{n} \right) D_{P_i} \quad (6)$$

where  $n$  is the number of floors and  $D_{P_i}$  is the global damage index of each floor. The damage index is normalized and expressed as a percentage.

Information on 60 hypothetical buildings, responding to the real characteristics of the buildings in the studied area was generated in a random manner by considering a uniform probability distribution law for the data. Each parameter required by the Italian methodology was qualified for each generated building. The vulnerability indices  $I_v$  were then calculated and a data file, containing all the necessary information for each building, was created to prepare the data for the next phase of the procedure. The structural analysis was performed using this data and as a result, the global damage indices  $D$  of the simulated buildings were determined for each macroseismic intensity. The simulation for the intensity VII, corresponding to the observed vulnerability function (Figure 1), was first carried out. With the points obtained, plotted in Figure 2, a regressional analysis was performed, whose result was the thick continuous curve shown in Figure 2, where the observed vulnerability function is also given. It should be noted that each point of Figure 2 corresponds to one or more buildings, due to the fact that it was possible to simulate buildings with similar vulnerability and damage indices.

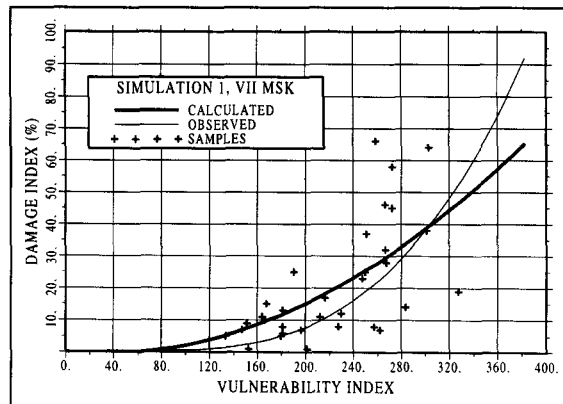


Figure 2 Simulated vulnerability function for intensity VII MSK (thick curve) and the observed vulnerability function (thin curve). Each point corresponds to at least one generated building.

The function fitted to the simulated points in Figure 2 is similar to the observed function within the vulnerability index range 0-100. However, for higher vulnerability index values, the shape of the simulated curve differs from the shape of the observed

curve. Two aspects must be considered here. Firstly, the observed function is based on real data and, therefore, can be considered the more reliable of the two. Secondly, the weights  $W_i$ , given in Table 1 and used in the evaluation of the vulnerability index (Equation 4), which were proposed by Benedetti and Petrini (1984), are based on a seismic damage assessment performed for Italian buildings. Taking into account these aspects, the calculated vulnerability function was calibrated from the observed function. The calibration strategy consisted of modifying the weights  $W_i$  without altering their proportionality relationship. This is required by the fact that the parameters of the vulnerability index method are arranged hierarchically using the mentioned relations. The calibration can be made by “carrying” the simulated function to the observed function, by means of the following process (Yépez, Barbat and Canas 1995):

- Considering as input data the values of the damage indices  $D$  for all the computer generated buildings, the vulnerability indices  $I_v$ , which these buildings would have if they corresponded to the observed function, are calculated. The computational process consists in obtaining for each building the roots of the third order polynomial that describes the observed vulnerability function (see Equation 5). As the value  $D$  of the damage index is known for each building, Equation (5) is solved to obtain the value  $I_v$ . In this process, only one of the roots is real, which means that the problem can be solved.
- Once the vulnerability index values  $I_v$  that belong to the hypothetical buildings are obtained, a mathematical process of conditional generalized inversion is applied. For this, the lineal system of equations generated by Equation (1) —one for each building—, in which  $I_v$  and  $K_i$  are known values, is used. Ten additional restriction equations, whose role is to maintain the original proportion between the weights  $W_i$ , are also used.
- As a result of the generalized inversion, new values of the weights  $W_i$  were obtained and used as input data in order to generate, by a new random process, new characteristics and properties of a further 60 buildings whose vulnerability indices were also then calculated. After evaluating the values of the new damage indices, a new regressional analysis —of the same order as the last— was performed, resulting in a new simulated vulnerability function. This curve is compared in Figure 3 with the observed one.
- It can be seen that the shape of both functions is very similar: between them there is only a shift, which suggests that the proposed calibration method can converge. Therefore, a new iteration was carried out, following the entire process described before: search of the polynomial roots, conditional generalized inversion and regressional analysis. From this new iteration, other values  $W_i$  were obtained, which are shown in Table 2, together with the corresponding values from the first iteration and the original values proposed by Benedetti and Petrini (1984).
- In the same way and with the new weights, other buildings were generated and the structural and regressional analysis were performed; the new simulated function is compared in Figure 4 with the observed function. The correlation coefficient of the



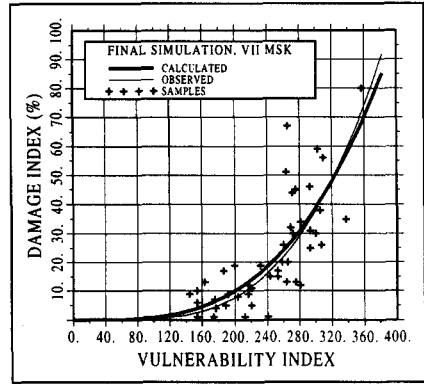
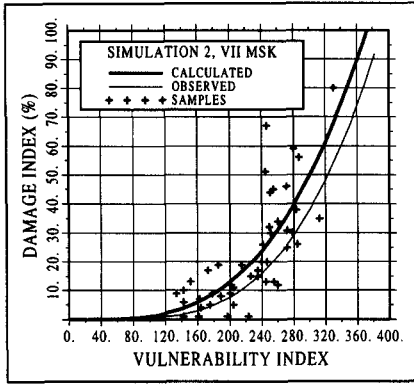


Figure 3 Second iteration in the simulation of the observed vulnerability function for intensity VII MSK and the comparison with the observed function.

Figure 4 Final iteration in the simulation of the observed vulnerability function for intensity VII MSK and the comparison with the observed function.

TABLE 2

Original  $W_i$  values of the scale proposed by Benedetti and Petrini (1984) and the  $W_i$  values obtained by iterative calibration.

Parameter $i$	Initial (Benedetti, Petrini)	Iteration 1	Iteration 2
1	1.00	1.015	1.095
2	0.25	0.254	0.274
3	1.50	1.523	1.643
4	0.75	0.762	0.821
5	1.00	1.015	1.095
6	0.50	0.508	0.548
7	1.00	1.015	1.095
8	0.25	0.254	0.274
9	1.00	1.015	1.095
10	0.25	0.254	0.274
11	1.00	1.015	1.095

polynomial regression corresponding to the simulated curve was about 90%, very similar to the correlation coefficient of the regression for the observed vulnerability function.

Obviously, the agreement between the two functions is excellent. If a better precision is desired, a new iteration can be made. However, the next two iterations produced weight values  $W_i$  different only in the fourth decimal, as compared with those of the second iteration. Consequently, has been considered that the convergence of the process and the calibration of the simulated function was achieved in the second iteration.

## PROBABILISTIC SIMULATION STUDY

In the simulation process described in the previous section, only 60 buildings were generated in order to simplify the regressional polynomial analysis and the generalized inversions necessary for the calibration. The formal simulation phase of the study is described in this section. Complete information for about 2000 hypothetical buildings was generated. The results of the analysis and the final polynomial regression for the intensity level VII MSK are shown in Figure 5. The correlation index was 80%, a value which can be considered sufficiently high. In many cases, one point of the figure corresponds to more than one building, because buildings with similar vulnerability and damage indices were generated.

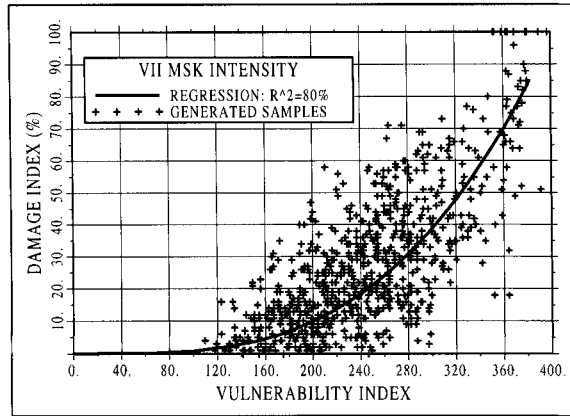


Figure 5 Final simulation process and polynomial regression for an intensity level VII MSK.

The Monte Carlo method (Rubinstein 1981) used in this simulation study consists of computing, by means of a deterministic structural analysis procedure, the results of many numerical experiments corresponding to randomly generated input data and searching for the probability distribution law that fits the histogram of the results. The first phase of this simulation process consisted of the random generation of the parameters involved in the evaluation of the vulnerability index, a process which was based on a uniform probability distribution law. Using the linear combination of the calibrated weights (Equation 4), the vulnerability indices were then obtained. A relative frequency histogram for all the generated vulnerability indices and the normal distribution density function have been plotted in Figure 6. Figure 7 shows the cumulative frequency histogram of the vulnerability indices, together with the corresponding distribution function. It can be seen that the data are closely approached by the normal distribution.

The probabilistic expression to calculate the specific seismic risk, involving the vul-

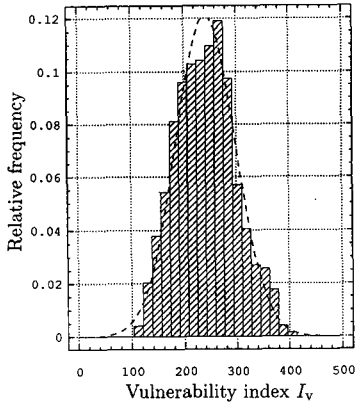


Figure 6 Histogram of the vulnerability index and the fitted normal distribution density function.

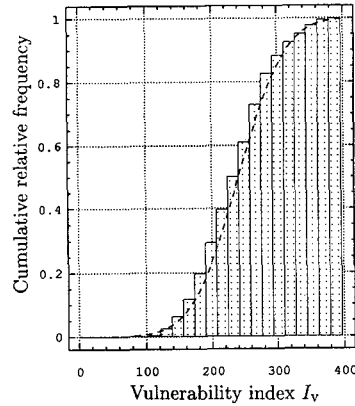


Figure 7 Cumulative frequencies of the vulnerability index and the fitted normal distribution function.

nerability index method, is

$$F(\bar{d}) = \int_0^{\bar{d}} \int_0^{I_{vmax}} \int_0^{I_{max}} f(d | I_v, I) f(I_v) f(I) dI dI_v dd \tag{7}$$

where  $F(\bar{d})$  is the damage cumulative distribution function for a fixed damage level  $d = \bar{d}$ ;  $f(d|I_v, I)$  is the conditional density function of damage over the vulnerability index  $I_v$  and the intensity  $I$ ;  $f(I_v)$  and  $f(I)$  are the density functions of  $I_v$  and  $I$ , respectively. The specific risk  $S$  is expressed by Equation (3). In Figures 6 and 7, the term  $f(I_v)$  is shown. Although it is obvious that the frequency histogram of the vulnerability index is well described by the normal distribution, the use of a significance contrast such as the  $\chi^2$  or the *Kolmogorov-Smirnov* test is required for a rigorous statistical analysis. To apply such tests, it is necessary to define a significance level, whose typical values lie between 0.01 and 0.05. Nevertheless, depending on the problem under consideration, a value equal to 0.10 is adequate (Karian and Dudewicz 1991). Usually, the significance level is represented as a percentage. Both tests have been applied to the vulnerability index histogram and it has been observed that the normal distribution fits the data with a significance level of 5%. In this way, the function  $f(I_v)$ , necessary to evaluate the specific seismic risk  $F(\bar{d})$  with Equation (7), has been defined.

The density function  $f(I)$  is obtained from hazard studies. It is possible to use, for example, a distribution derived from the relation between the number of annual events of intensity equal to or higher than a value  $I$  and an intensity  $I$ . The intrinsic probability can also be calculated from seismic hazard maps which include the corresponding return period. In any case,  $f(I)$  is a known term of Equation (7). The last step is to determine the term  $f(d | I_v, I)$ , which represents the conditional damage density function for  $I_v$  and  $I$ .

Benedetti, Benzoni and Parisi (1988) have observed that, for a specified range of values  $\Delta I$  and  $\Delta I_V$ , the conditional damage distribution tends to a normal distribution, which allows Equation (7) to be discretized. In this way, the conditional damage probability  $P[d | \Delta I_V, \Delta I]$  is obtained as a damage probability matrix—to be precise, a threedimensional array—, due to the inclusion of the parameter  $I_V$ . Thus, Equation (7) can be discretized as follows:

$$P[d_i < d < d_{i+1}] = \sum_{k=1}^n \sum_{j=1}^m P[d_i < d < d_{i+1} | I_{V_j} < I_V < I_{V_{j+1}}, I_k < I < I_{k+1}] \quad (8)$$

$$\times P[I_{V_j} < I_V < I_{V_{j+1}}] \times P[I_k < I < I_{k+1}]$$

where  $P[d_i < d < d_{i+1}]$  is the damage probability within the interval  $(d_i, d_{i+1})$ . The first factor in the right-hand side member is the conditional probability of the damage over the vulnerability index and the macroseismic intensity. The other two factors represent the total probability for both the vulnerability index and the intensity.  $m$  and  $n$  are the total number of the intervals  $\Delta I_V$  and  $\Delta I$ , respectively. In the simulation performed for the intensity level VII MSK, the values  $k$  and  $n$  in Equation (8) are equal to 6.

The vulnerability index scale was subdivided in band-width intervals equal to 50. By using all the values of the damage indices  $D$  corresponding to the buildings with a vulnerability index within a specified band-width, a frequency histogram was produced. After that, the possible probabilistic models which can be fitted to the histograms and can pass the contrast tests with a 5% significance level or, in extreme cases, with a 10% significance level, have been considered. Figures 8 and 9 present some examples of the mentioned histograms with the fitted probabilistic models.

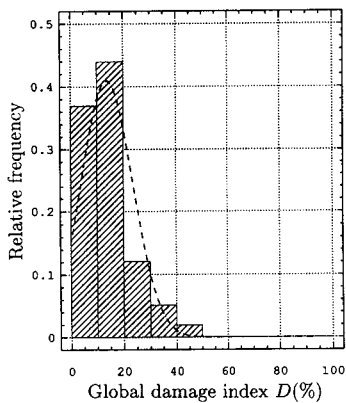


Figure 8 Histogram and normal damage distribution.  $I_V \in [150, 200]$  and  $I =$  VII MSK.

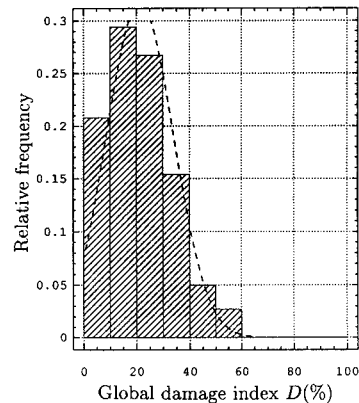


Figure 9 Histogram and normal damage distribution.  $I_V \in [200, 250]$  and  $I =$  VII MSK.

Analysing the histograms, the normal distribution turned out to be the model which best fitted the results in all cases, with the exception of the case  $I_V > 350$  in which the

Kolmogorov-Smirnov test passed but the  $\chi^2$  test did not. For this case, the lognormal distribution was the chosen model. Once the simulated data were fitted by a model, the damage density function conditioned by  $I_v$  and  $D$  could be evaluated by estimating the density function of the fitted models. If  $f(I)$  is available from seismic hazard studies, the triple integral of Equation (7) can be calculated, replacing the models obtained for the damage index,  $f(d | I_v, I)$ , for the vulnerability index,  $f(I_v)$ , and for the macro-seismic intensity,  $f(I)$ , in order to perform the convolution and then to evaluate the specific seismic risk. Nevertheless, with the aim of increasing the velocity of the numerical evaluation process, Equation (8) was discretized and probability matrices for the discretized ranges were then obtained, calculating the corresponding density functions of the models. Thus, the convolution process was converted into a simpler operation series by means of the following steps:

- The values of Table 3 were obtained by discretizing the density function of the vulnerability index.

TABLE 3

Discretized values of  $f(I_v)$  for the model fitted to the simulated data using the normal distribution law.

range of $I_v$	$f(I_v)$
0 – 100	0.0064
100 – 150	0.0475
150 – 200	0.1795
200 – 250	0.3273
250 – 300	0.2885
300 – 350	0.1229
> 350	0.0228

- The matrix of Table 4 can be obtained by discretizing the density functions of the models fitted to the damage indices. On the horizontal axis, the damage index ranges used in the discretization process, whose band-width is 20%, are placed. The corresponding vulnerability index ranges are displayed on the vertical axis.

Another way to express  $f(d | I_v, I)$  in a continuous form is shown in Figure 10 for the intensity level VII MSK. In this figure, the cumulative probability of the global damage index conditioned by  $I_v$  is described by means of *fragility curves* for the fitted models.

Once the simulation process for the intensity VII MSK had been carried out, several simulations for the intensity levels VI, VIII and IX MSK were performed. The computation process for these cases is similar to the first case with the exception that there is no observed function available to calibrate the simulated functions. However, the calibrated weights  $W_i$  obtained during the simulation performed for level VII MSK, were used in all the remaining cases and, therefore, the expected results are simulated

TABLE 4  
 Discretized values of  $f(d | I_v, I)$  for the model  
 fitted to the simulated data for I=VII MSK.

$f(d   I_v, I)$	0 – 20	20 – 40	40 – 60	60 – 80	80 – 100
0 – 100	1.000	0.000	0.000	0.000	0.000
100 – 150	0.838	0.008	0.000	0.000	0.000
150 – 200	0.660	0.257	0.004	0.000	0.000
200 – 250	0.413	0.473	0.068	0.001	0.000
250 – 300	0.183	0.455	0.293	0.048	0.002
300 – 350	0.005	0.344	0.467	0.149	0.029
> 350	0.000	0.000	0.015	0.276	0.467

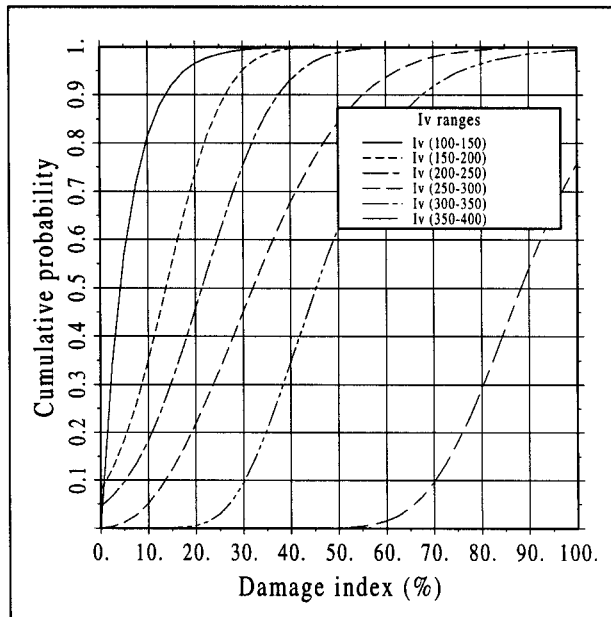


Figure 10 Fragility curves for different vulnerability index ranges. Intensity level VII MSK.

functions which adequately represent the phenomenon for the new intensities. The final results are shown in Figure 11. All the simulated curves are polynomial regressions with the following form:

$$D(\%) = a_1 + a_2 I_v + a_3 I_v^2 + a_4 I_v^3 \tag{9}$$

The regression coefficients and the correlation indices are presented in Table 5.

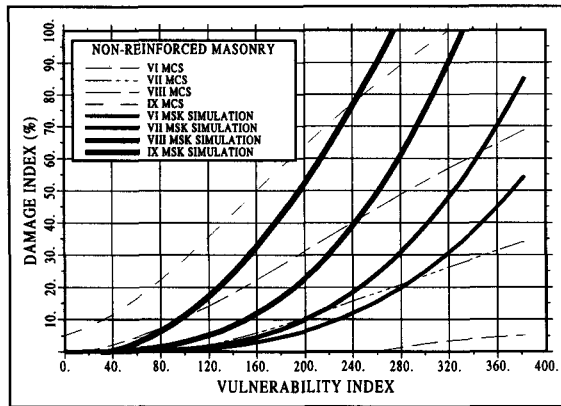


Figure 11 Vulnerability functions for the simulated unreinforced masonry buildings for different MSK intensity levels. The thin non-continuous lines represent the Italian functions proposed by Angeletti *et al.* (1988).

TABLE 5

Coefficient values of the polynomial regressions and obtained correlation indices.

Intensity	$a_1$	$a_2$	$a_3$	$a_4$	Correl.
VI	0.02	0.00115144	-0.00007704	0.00000117	80%
VII	0.02	0.00396271	-0.00014492	0.00000187	89%
VIII	-0.10	-0.00112200	0.00007070	0.00000254	88%
IX	-0.78	-0.03608463	0.00161535	-0.00000053	91%

Tables 6, 7 and 8 show the discretized values of the conditional density function of the damage for a specified vulnerability index range and for the corresponding intensity level *I* (similar to Table 4), with the same range of values as were considered before.

Each value in Table 3 represents the probability of obtaining a value of the vulnerability index between the given upper and lower limits. In Table 4, the values represent the probabilities of obtaining a damage index between two levels, conditioned by a value of the vulnerability index within a specific range, whenever earthquake intensity exceeds level VI and reaches level VII in the MSK scale.

If the discretized values of the density function of the intensity between levels VI and VII MSK for some return period are available, the complete solution of Equation (8) can be worked out as a series of cumulative products. It is possible to express these results, for example, in the following way: “there is a 30% probability of a damage level between 20% and 40% occurring in unreinforced masonry structures whose vulnerability indices are higher than 200 but lower than 250 in the event of an earthquake exceeding

TABLE 6

Discretized values of  $f(d | I_v, I)$  for the model fitted to the simulated data for I=VI MSK.

$f(d   I_v, I)$	0 – 20	20 – 40	40 – 60	60 – 80	80 – 100
0 – 100	1.000	0.000	0.000	0.000	0.000
100 – 150	1.000	0.000	0.000	0.000	0.000
150 – 200	1.000	0.000	0.000	0.000	0.000
200 – 250	0.731	0.223	0.007	0.000	0.000
250 – 300	0.421	0.522	0.038	0.000	0.000
300 – 350	0.119	0.728	0.143	0.010	0.001
> 350	0.000	0.027	0.608	0.340	0.025

TABLE 7

Discretized values of  $f(d | I_v, I)$  for the model fitted to the simulated data for I=VIII MSK.

$f(d   I_v, I)$	0 – 20	20 – 40	40 – 60	60 – 80	80 – 100
0 – 100	1.000	0.000	0.000	0.000	0.000
100 – 150	0.976	0.002	0.000	0.000	0.000
150 – 200	0.540	0.409	0.015	0.000	0.000
200 – 250	0.124	0.244	0.285	0.198	0.082
250 – 300	0.010	0.083	0.280	0.377	0.203
300 – 350	0.000	0.000	0.000	0.115	0.813
> 350	0.000	0.000	0.000	0.000	1.000

TABLE 8

Discretized values of  $f(d | I_v, I)$  for the model fitted to the simulated data for I=IX MSK.

$P(d   I_v, I)$	0 – 20	20 – 40	40 – 60	60 – 80	80 – 100
0 – 100	1.000	0.000	0.000	0.000	0.000
100 – 150	0.445	0.555	0.000	0.000	0.000
150 – 200	0.068	0.263	0.389	0.221	0.048
200 – 250	0.000	0.000	0.024	0.447	0.496
250 – 300	0.000	0.000	0.000	0.000	1.000
300 – 350	0.000	0.000	0.000	0.000	1.000
> 350	0.000	0.000	0.000	0.000	1.000

the intensity VI MSK (but not the intensity VII MSK) and having a return period of 50 years". The same type of result, for other intensities, is included in tables 6, 7 and 8.

Depending on the considered discretization ranges, it is also possible to express the results in terms of cumulative probability. One example would have this form: "there is an 80% probability of damage levels under 70% occurring in unreinforced masonry



buildings whose vulnerability index values are within the range 200-300 in the event of an earthquake exceeding the intensity VIII MSK (but not the intensity IX MSK) and with a return period of 500 years”.

Another possibility for assessing the seismic risk is the use of damage scenarios. These are graphic schemes of the convolution process, which show all the possible average damage levels in an urban zone, by using similar vulnerability functions to those obtained in this study (Figure 11) for the macroseismic intensities specified for the expected earthquakes. The occurrence probabilities of the mentioned scenarios are related to the return period of the mentioned earthquake intensity.

### APPLICATION TO THE “EIXAMPLE” IN BARCELONA, SPAIN

The developed methodology has been used to investigate the vulnerability of the unreinforced masonry buildings located in the “Eixample”, a central urban zone of Barcelona, and to simulate probable damage scenarios in this area. The analyzed sample includes 9 blocks in which there are 181 brick masonry structures —built between 1860 and 1939— and 35 buildings having other typologies (concrete or steel buildings, churches, etc.). Only the brick masonry buildings have been considered in this study. The average number of floors, total height and floor area are 6, 19 m and 281 square meters, respectively. An example of a typical block of the “Eixample” can be seen in Figure 12. The procedure used to perform the study consists, basically, of the three following tasks:

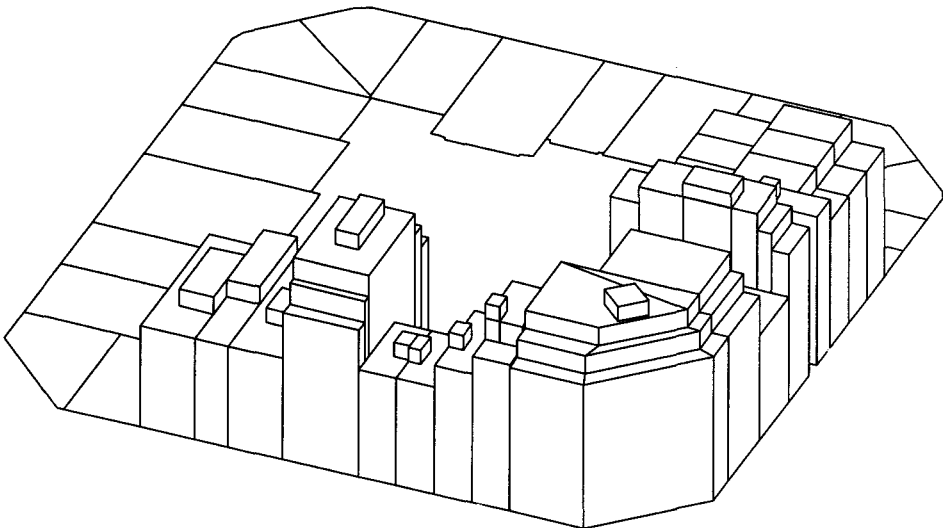


Figure 12 Example of a typical block of the “Eixample”.

- 1.- The first phase includes the gathering of the necessary information. A digital map of the area under study was obtained from the Barcelona Cartographic Center which contained such information as: floor area, height, limits, plant shape and mailing address of the buildings. From the available drawing plans found in the historic archives of the city the required structural characteristics of the buildings were obtained.
- 2.- In the second phase, the data obtained in the first phase were used to deduce all the parameters required by the methodology; by inspecting each building, the information was checked and completed. Finally, the buildings were organized in a random manner, constituting blocks similar to the real ones.
- 3.- In the final phase, computer programs implemented in a Geographical Information System (G.I.S.) were used to perform a simple management of the data, to carry out the necessary calculations and to plot the results which represent damage scenarios according to given intensity levels. The vulnerability functions obtained before (Figure 11) were used to estimate probable average damages to the buildings.

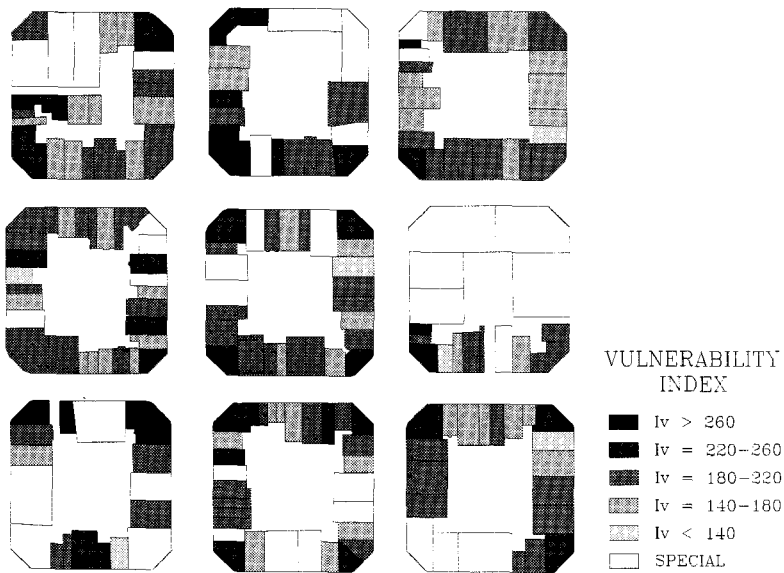


Figure 13 Vulnerability map of the studied area of the “Eixample”.

The final results obtained for the studied area have been represented graphically in the form of maps and frequency histograms. In the map in Figure 13, the vulnerability index of each studied building is shown for five different ranges of values: low ( $I_v \leq 140$ ), medium-low ( $140 < I_v \leq 180$ ), medium ( $180 < I_v \leq 220$ ), high ( $220 < I_v \leq 260$ ) and very high ( $I_v > 260$ ). The importance of this map within the frame of the defined scale is

that it permits the most vulnerable buildings to be identified. Thus, it may be observed that there are 41 buildings (23%) which have high or very high vulnerability values. These buildings require more detailed studies before any decision is taken regarding the possible reduction of the seismic risk in the studied area.

Figures 14, 15 and 16 show three possible damage scenarios for three different earthquake intensities. In these figures, five ranges of the mean damage index  $D$  can be identified: low damage ( $D \leq 20\%$ ), moderate damage ( $20\% < D \leq 40\%$ ), high damage ( $40\% < D \leq 60\%$ ), very high damage ( $60\% < D \leq 80\%$ ) and collapse ( $D > 80\%$ ).



Figure 14 Damage scenario for an earthquake of intensity VII MSK.

Figure 17 shows the frequency distribution of the vulnerability index in the area. It can be seen that the vulnerability index has mainly medium and high values. Although the buildings of the area are relatively regular in terms of plant and elevation, the high values of their vulnerability indices are decisively influenced by the low quality of the materials and by the medium-low preservation state. Similarly, figures 18, 19 and 20 show the frequency distribution of the damage index; it can be seen that the average damage increases in a non-proportional way with the increment of the intensity level.

For the intensity level VII MSK, most of the buildings suffer damages between 10% and 20%, whilst 5% have a damage index between 20% and 30%. Only 8% of the buildings would suffer low damage (up to 5%). It has to be emphasized that the studied urban area belongs to a moderate seismic region, a fact that is confirmed by

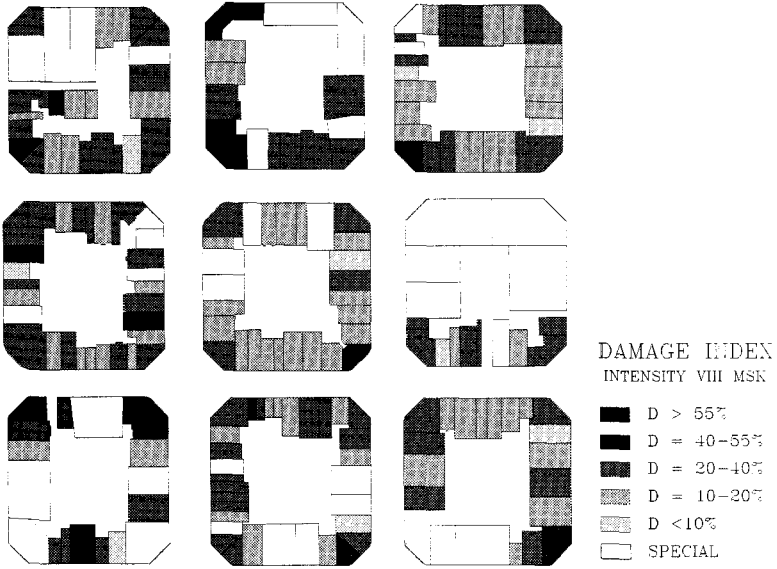


Figure 15 Damage scenario for an earthquake of intensity VIII MSK.

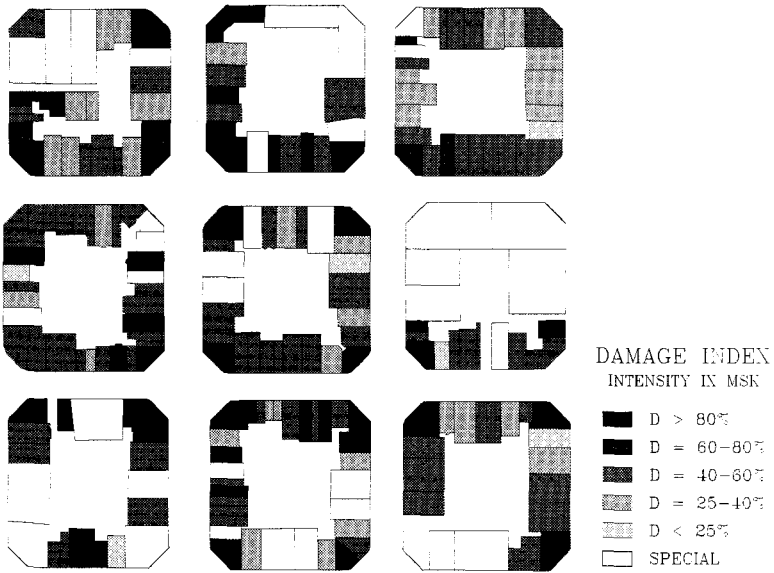


Figure 16 Damage scenario for an earthquake of intensity IX MSK.

the Spanish Seismic Code which stipulates for Barcelona, for medium soil, the intensity level VII MSK. For the intensity VIII MSK, important damage can be observed, mainly between 20% and 40% and, in some cases, exceeding 40%. For the intensity IX MSK, the damage is very high: 72% of the buildings show a damage level over 40%, with the predominant values between 50% and 60%. A detailed cost-benefit study of a possible reparation is required in this case. Nevertheless, the expected reparation costs would probably be excessively high.

Finally, Figure 21 shows the parameters involved in the evaluation of the vulnerability index for the buildings of the studied area and their qualifications  $K_i$ . This figure is useful because it permits the parameters which most influence the vulnerability of the buildings to be identified. Thus, it can be seen that parameters 3, 5, 6 and 8, corresponding to the conventional resistance, floor system, plant configuration and maximum distance between bearing walls, respectively, are the most important and, therefore, efforts to limit the vulnerability must be focussed these parameters.

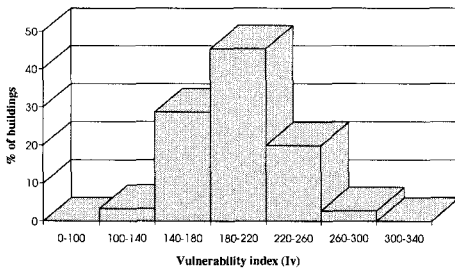


Figure 17 Frequency histogram of the vulnerability index.

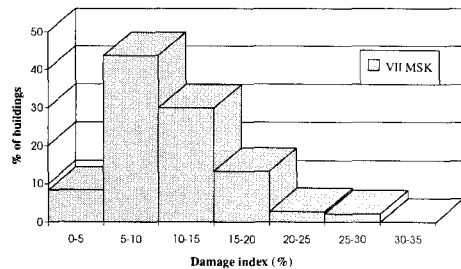


Figure 18 Frequency histogram of the damage index for I=VII.

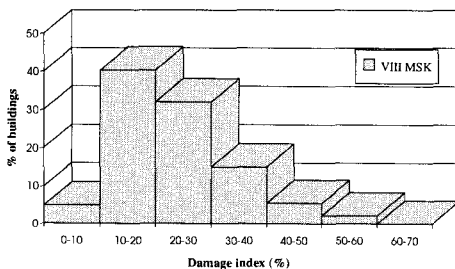


Figure 19 Frequency histogram of the damage index for I=VIII.

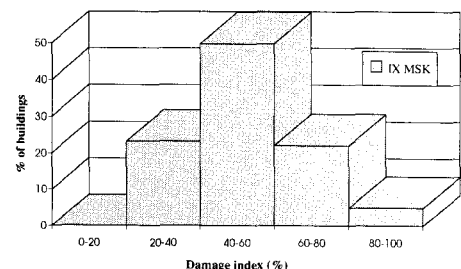


Figure 20 Frequency histogram of the damage index for I=IX.

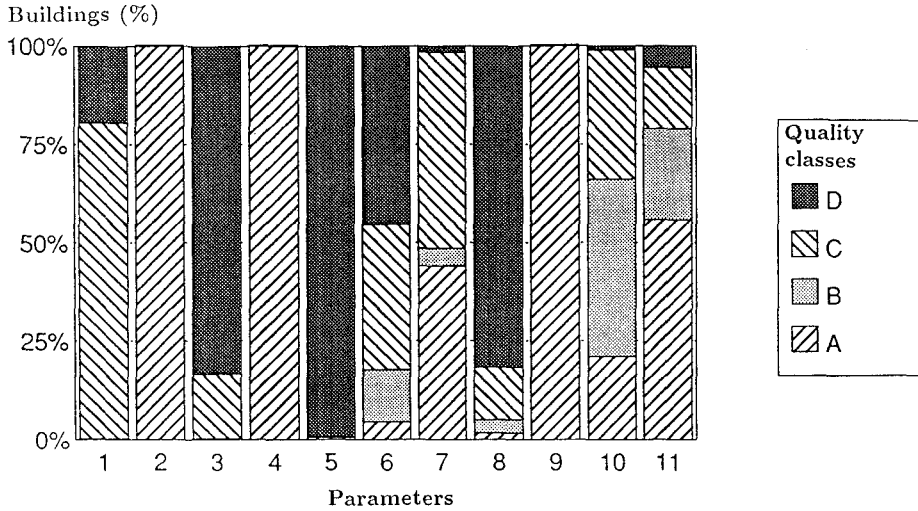


Figure 21 Parameters involved in evaluating the vulnerability index of the buildings in the studied area.

## CONCLUSIONS

This paper presents a computer simulation of the damage to buildings and its probabilistic evaluation, based on a vulnerability curve obtained from a post-earthquake damage survey. The results—the first of this type obtained in Spain—permit the estimation, with a certain probability level, of the expected damage to buildings from an earthquake of a given intensity, as well as also enabling to take decisions aiming to reduce the seismic risk in a zone. For example, strengthening of some specific structures can considerably decrease their vulnerability index, resulting in a reduction of the vulnerability index in the area. Consequently, the damage levels, or the probabilities of high damage values for earthquakes of the same intensity and the same return period, will be reduced. At the same time, the results of the study can be multiplied by costs, giving, thus, the probable economic losses—complete seismic risk—together with their respective occurrence probabilities. Such a result is important in taking decisions on the suitability of rehabilitate or demolish a structure.

For the specific seismic risk assessment in an urban zone, it is necessary to obtain both the vulnerability distribution of the buildings in the area and the distribution of the macroseismic intensity. Starting from these data, it is possible to fit probabilistic models and to perform the convolution of the probability density functions. Their discretized form can also be used. In the latter case, the conditional density function values of the damage corresponding to different earthquake intensities can be applied as three-dimensional damage probability matrices with damage levels, vulnerability index ranges and macroseismic intensities. If a data base relative to the economic cost of the structures in risk is available, a total seismic risk study of the zone can be performed.

In this study, computer simulation has partially replaced the information that could be obtained from post-earthquake survey studies. The simulation of many hypothetical buildings has been possible because the model used for unreinforced masonry was relatively simple. However, it has to be emphasized that damage survey studies are always necessary to calibrate the numerical results and/or to verify the calibration of the vulnerability functions.

Finally, the effectiveness of the proposed methodology has been demonstrated by simulation of mean damage scenarios for an area of central Barcelona and possible damage levels for earthquakes of different intensities have been quantified. The most vulnerable buildings of the area have also been identified, together with those structural characteristics which mostly increase their vulnerability index. If the mitigation of the seismic risk is required, efforts must be focussed on reducing the values of the mentioned characteristics.

## REFERENCES

- Abrams, D. P. (1992). "Strength and behaviour of unreinforced masonry elements", *Proceedings of the Tenth World Conference on Earthquake Engineering*, Madrid, **7**, 3475-3480.
- Angeletti, P., Bellina, A., Grandori, E., Moretti, A. and Petrini, V. (1988). "Comparison between vulnerability assessment and damage index, some results", *Proceedings of the Ninth World Conference on Earthquake Engineering*, Tokyo, **7** 181-186.
- Benedetti, D. and Petrini, V. (1984). "Sulla vulnerabilità sismica di edifici in muratura i proposte di un metodo di valutazione", *L'industria delle Costruzioni*, **149**, 66-74.
- Benedetti, D., Benzoni, G. and Parisi, M. (1988). "Seismic vulnerability and risk evaluation for old urban nuclei", *Earthquake Engineering and Structural Dynamics*, **16**(2), 183-201.
- Chung, Y. S. and Shinozuka, M. (1988). *Automatic Seismic Design of Reinforced Concrete Buildings*, National Center for Earthquake Engineering Research, State University of New York at Buffalo, Buffalo, NCEER-88-0024.
- European Seismological Commission (1993). *European Macroseismic Scale 1992*, Cahiers du Centre Européen de Géodynamique et de Séismologie, Luxembourg, (Grünthal, G., editor), **7**.
- GNDT (1986). *Istruzioni per la Compilazione della Scheda di Relivamento Esposizione e Vulnerabilità Sismica Degli Edifici*, Gruppo Nazionale per la Difesa dai Terremoti, Regione Emilia Romagna y Regione Toscana.
- Goula, X., Olivera, C., Susagna, T. and Yépez, F. (1994). *Visita de Reconeixement a la Regió de Berja-Adra (Almería), afectada pels Sismes dels dies 23.12.1993 i 4.1.1994*, Departament de Política Territorial i Obres Públiques, Servei Geològic de la Generalitat de Catalunya, Barcelona, GS-042-94.
- Karian Z. and Dudewicz, E. (1991). *Modern Statistical Systems and GPSS Simulation*, Computed Science Press, New York.
- Manfredi, G., Mazzolani, S. and Masi, A. (1992). "Review of existing in experimental testing of masonry structures subjected to horizontal loads", *Proceedings of the Tenth World Conference on Earthquake Engineering*, Madrid, **6**, 3557-3562.

- Rubinstein, R. Y. (1981). *Simulation and Monte Carlo Method*, John Wiley & Sons, New York.
- Sandi, H. (1986). "Vulnerability and risk analysis for individual structures and systems", *Proceedings of the 8th European Conference on Earthquake Engineering*, Lisbon, 7, 11-60.
- Yépez, F., Barbat, A. H. and Canas, J. A. (1994). *Riesgo, peligrosidad y vulnerabilidad sísmica de edificios de mampostería*, International Center for Numerical Methods in Engineering, CIMNE, Barcelona, monograph IS-12.
- Yépez, F., Barbat, A. H. and Canas, J. A. (1995). *Simulación de escenarios de daño para estudios de riesgo sísmico*, International Center for Numerical Methods in Engineering, CIMNE, Barcelona, monograph IS-14.
- Yépez, F., Canas, J. A., Barbat, A. H., Roca, A. and Goula, X. (1995). "Seismic vulnerability evaluation in urban areas from observed damage", *Proceedings of the Fifth International Conference on Seismic Zonation*, Nice, 1, 109-116.